ISSN 8756-6990, Optoelectronics, Instrumentation and Data Processing, 2013, Vol. 49, No. 2, pp. 178–183. © Allerton Press, Inc., 2013.
Original Russian Text © I.I. Guzhov, S.P. Il'inykh, R.A. Kuznetsov, A.R. Vagizov, 2013, published in Avtometriya, 2013, Vol. 49, No. 2, pp. 85–91.

ANALYSIS AND SYNTHESIS OF SIGNALS AND IMAGES

Solution of the Problem of Phase Ambiguity by Integer Interferometry

I. I. Guzhov, S. P. Il'inykh, R. A. Kuznetsov, and A. R. Vagizov

Novosibirsk State Technical University,
pr. Karla Marksa 20, Novosibirsk, 630092 Russia
E-mail: vig@edu.nstu.ru

Received May 22, 2012

Abstract—An automatic method is proposed to resolve phase ambiguity in interpreting fringe patterns by a series of two phase distributions with different periods. The method does not require identification of local phase transitions in adjacent image regions and can determine the total phase at each point separately.

Keywords: optics, interferometry, phase-shifting interferometry, resolution of phase ambiguity.

DOI: 10.3103/S8756699013020106

INTRODUCTION

Determining the three-dimensional profile of objects is one of the most important problems of technical measurements. The most widely used methods are based on the projection of structured light onto the surface of the object [1–7]. The error in determining the profile can be significantly reduced by projection of a series of patterns with a sinusoidal fringe profile, in which each sinusoidal pattern is shifted by a known amount. This approach is widely used in interference measurements and is called the method of interferometry with an incremental phase shift [8]. The basic resolving equations obtained for this method are also used to determine the profiles of objects in projection methods of measurement.

The main task of interpretation is to calculate the phase difference $\varphi(x, y)$ from the recorded intensities $I_i(x, y)$. For different phase shifts δ_i, the intensity of light reflected from an object can be represented as

$$I_i(x, y) = A_0(x, y)(1 + V(x, y)\cos(\varphi(x, y) + \delta_i)), \quad (1)$$

where $A_0(x, y)$ is the average brightness; $V(x, y)$ is the image contrast; $i = 1, 2, \ldots, m$ (m is the number of phase shifts).

A generalized interpretation algorithm which enables one to find the value of the phase distribution $\varphi(x, y)$ for known values of δ_i is given in [9–11]. The surface profile of the object is given by the obtained phase distribution taking into account the geometric parameters of the measuring system [12].

However, the periodicity of the phase of the projected fringes limits the height range in the determination of the profile. This gives rise to the so-called phase ambiguity. A common way used to eliminate this problem is based on adding (or subtracting) multiples of 2π to the measured phase values calculated up to the period. In this case, a number of problems arise.

The process of identifying phase transition jumps requires an element-by-element comparison of phases at adjacent points of the phase field. In the presence of noise, false phase transitions occur. Erroneous detection of a phase transition leads to the spread and accumulation of errors across the field of the unwrapped image, leading to inaccurate interpretation of the reconstructed phase profile.

This problem is solved using various methods of local and global optimization, theory of signal and image processing, dynamic programming, statistical approaches to estimating the probability of phase transitions,

exhaustive search and heuristic algorithms, artificial intelligence, etc. [13]. One way to solve this problem is to combine different methods [14].

The purpose of this work was to develop a new method for resolving phase ambiguity by analyzing the distribution of phase values for different periods of the projected fringes that does not require the detection of local phase transitions in adjacent image regions.

DESCRIPTION OF THE METHOD AND EXPERIMENTAL RESULTS

The method of determining the absolute values of a measured quantity from the values of several measurements within a specified period is given in [15]. We consider an algorithm for measuring the absolute value of the phase using two different periods. Let these periods have values $m_1 = 5$ and $m_2 = 3$. The initial data are the results of measurements of the same quantity L for different values of the period (b_1 and b_2).

Because the results of the measurements are determined up to the period, for each set of two measurements there is a possible set of solutions which consists of a vertical column of points separated from each other by the value of the period. In Fig. 1, they are marked by squares for measurements with a period of 5 and by pluses for measurements with a period of 3.

The set of values that satisfy all sets specifies the range of the desired absolute value. Since the result of different measurements should be the same, all differing values are discarded.

Plotting the values of b_1 and b_2 (see Fig. 1) measured within the period of unambiguity on the vertical and horizontal axes, we obtain a table whose values satisfy the absolute values of the desired measured quantity. The absolute value of L is a solution of the system of comparisons

$$\begin{cases} L \equiv b_1 \bmod(m_1), \\ L \equiv b_2 \bmod(m_2). \end{cases} \tag{2}$$

The solutions of system of comparisons (2) for $L \in (0 \dots m_1 m_2 - 1)$ for $m_1 = 3$ and $m_2 = 5$ are shown in the table. The maximum range of the unambiguous determination of the absolute values is specified by the largest relative prime factor in the value of the period (3 and 5 are relative primes, the maximum range of determination $3 \cdot 5 - 1 = 14$). We have found a method based on well-known Chinese remainder theorem of the theory of integers [16], which allows one to analytically find the values of the Table [9]. Therefore, the method was called the integer method of resolving phase ambiguity.

Limiting the maximum range of measurements will lead to the appearance of sparse diagonals in the table (Fig. 2). The absolute values falling within the selected range will lie on these diagonals, and the values between the diagonals will be located outside this range (in the table, the allowed absolute values for this case are in bold).

As is evident from the figure, the values of b_1 and b_2 are located successively on the main diagonals. When the measurement error of b_1 and b_2 is ± 1, the difference between values of the absolute quantity L is

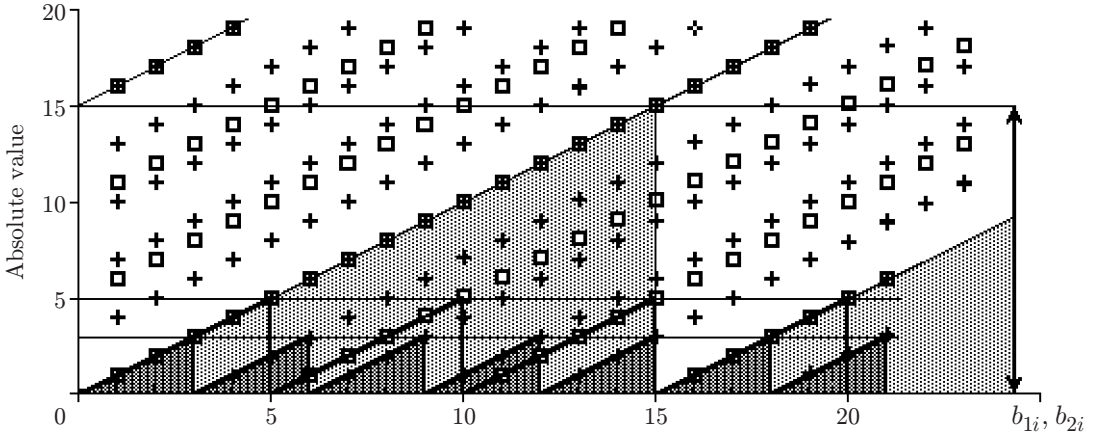

Fig. 1. Determination of the absolute value from the results of two measurements (b_1, b_2) for different periods ($m_1 = 5$ and $m_2 = 3$).

b_1	b_2		
	0	1	2
0	**0**	10	5
1	6	**1**	11
2	12	7	**2**
3	**3**	13	8
4	9	**4**	14

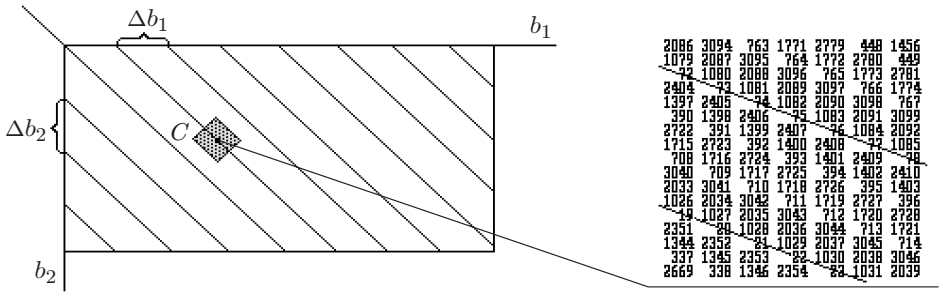

Fig. 2. Table of solutions with absolute values $m_1 = 53$ and $m_2 = 63$ and the enlarged part of the table with numerical values.

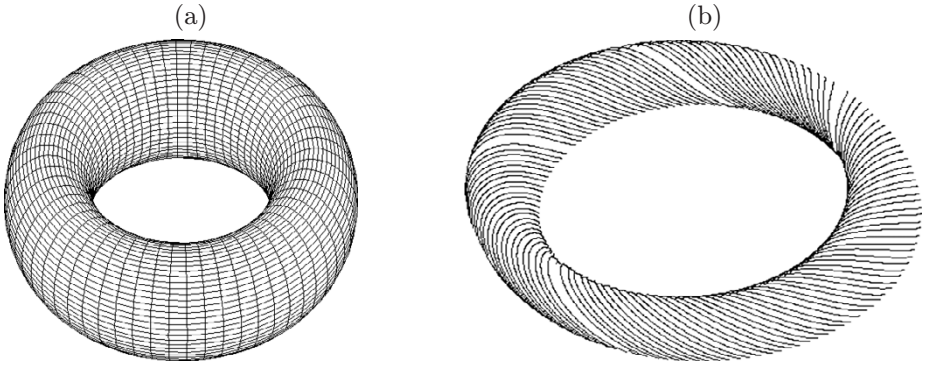

Fig. 3. Torus formed by joining the table of solutions: (a) table of solutions transformed into a torus, (b) diagonals on the surface of the torus with a limitation of the maximum range.

larger. To correctly determine L, it is necessary that the error of the initial data does not exceed half the distance between the diagonals. In real systems, it is difficult to satisfy these requirements; therefore, the method has not been widely used.

If we connect the continuations of the diagonals with a sequential increase in the numbers, we can see that the joining of the top and bottom horizontal lines and the left and right columns forms a torus (Fig. 3a). In the case of limitation of the measurement range, the possible comparison solutions form a spiral in the form of a thread on the surface of the torus (Fig. 3b). This allows us to adjust the position of a point on the torus. If a point on the surface of the torus does not belong to the spiral, it is likely that the correct value is on the turn of the thread line the closest to the point. For correction, it is necessary to determine the coordinates of this line on the surface of the torus and to project this point onto it.

The method was demonstrated on the projection setup shown schematically in Fig. 4a. A conical plastic container was used as the object. To eliminate distortions in projecting sinusoidal patterns, we used an original method [17]. A series of eight binary images of size 1024×768 pixels was projected onto the object using a Panasonic PT-D5500E DLP-projector (Fig. 4b). Each image contained 1 bit of a byte representation of the brightness field of the projected sinusoidal grating. Then, the images reflected from the object were sequentially entered into a computer using a Canon 550 camera (frame size 4752×3168 pixels) and united into an image of the grayscale sinusoidal grating [18] (see Fig. 4b). To determine the phase profile of the object, two series of sinusoidal gratings with a phase shift of 0, 120, and 240° were projected. The lattice period in the resolution elements was $m_1 = 167$ for the first series and $m_2 = 241$ for the second series.

As a result of interpretation of the images, the phase distributions $\varphi_1(x, y)$ for the lattice period m_1 (Fig. 5a) and $\varphi_2(x, y)$ for the period m_2 (Fig. 5b) were calculated.

Further interpretation is performed as follows:

1. We normalize the phase distributions $\varphi_1(x, y)$ and $\varphi_2(x, y)$ shown in Fig. 5:

$$b_i = \text{int}\left(\frac{m_i}{2\pi}\,\varphi_i\right), \quad i = 1, 2, \ldots . \tag{3}$$

The field $\varphi_1(x, y)$ will have values of 0 to $m_1 - 1$ and $\varphi_2(x, y)$ of 0 to $m_2 - 1$. We compose a table similar

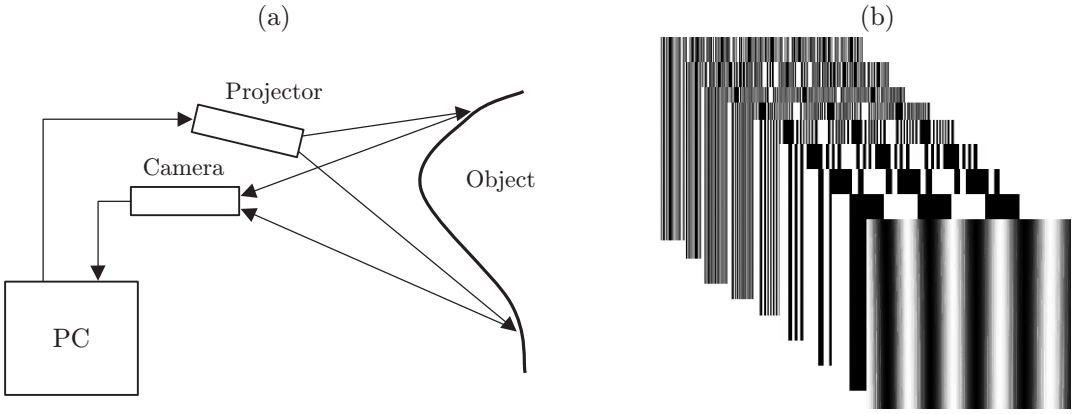

Fig. 4. Demonstration of the method: (a) diagram of the experimental setup, (b) bit expansion of the sinusoidal pattern.

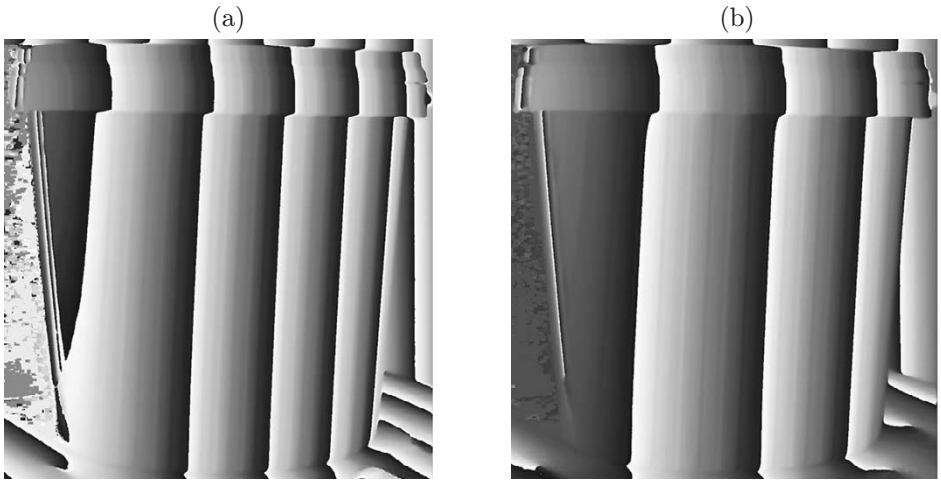

Fig. 5. Phase fields with periods: $m_1 = 167$ (a) and $m_2 = 241$ (b).

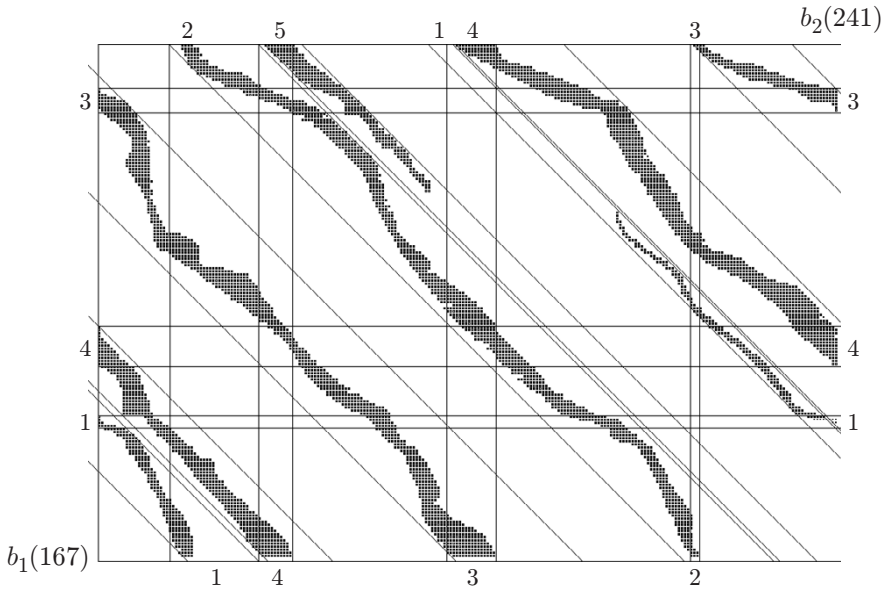

Fig. 6. Table of solution trajectories.

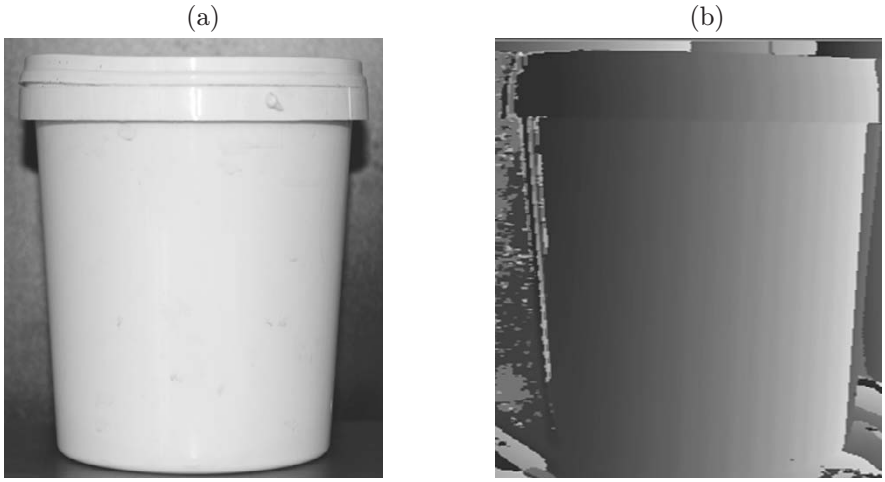

Fig. 7. Results of the experiment: (a) photograph of the object, (b) its reconstructed three-dimensional profile (intensity values correspond to the values of the z coordinates of the profile).

to the table in Fig. 2. To do this, we plot in it all values of the normalized phase fields $\varphi_1(x, y)$ and $\varphi_2(x, y)$ (Fig. 6).

2. We combine the diagonal into one strip using the joining of the table into a torus (see Fig. 3b) and number the fringes. (The fringe numbers are shown on the horizontal and vertical axes.)

3. To determine the absolute values, we add the values of the period multiplied by the number of this fringe to the normalized values phase $\varphi_1(x, y)$ and $\varphi_2(x, y)$ to.

Figure 7a shows the measured object, and Fig. 7b its three-dimensional profile reconstructed by the stated algorithm.

CONCLUSIONS

A fully automated method for resolving phase ambiguity for phase distributions with different periods was proposed. The method is independent of the spatial distribution of the phase information (profile and arrangement of interference fringes), is fairly stable, and can be used for noncontact measurements of the surface profile of objects.

This work was supported by the Ministry of Education and Science of Russian Federation (Project No. 7.599.2011).

REFERENCES

1. D. L. Andrews, *Structured Light and Its Applications. An Introduction to Phase-Structured Beams and Nanoscale Optical Forces* (Academic Press, 2008).
2. G. Rajshekhar, S. S. Gorthi, and P. Rastogi, "Estimation of Dynamically Varying Displacement Derivatives using Fringe Projection Technique," Appl. Opt. **50** (3), 282–286 (2011).
3. Y. Wang, K. Liu, D. L. Lau et al., "Maximum SNR Pattern Strategy for Phase Shifting Methods in Structured Light Illumination," JOSA A. **27** (9), 1962–1971 (2010).
4. F. M'erideau, L. A. S. Secades, and G. Eren, et al., "3-D Scanning of Nonopaque Objects by Means of Imaging Emitted Structured Infrared Patterns," IEEE Trans. Instrum. Meas., **59** (11), 2898–2906 (2010).
5. E. Steger and K. N. Kutulakos, "A Theory of Refractive and Specular 3D Shape by Light-Path Triangulation," Intern. Journ. Comput. Vis. **76** (1), 13–29 (2008).
6. T. Peng and S. K. Gupta, "Model and Algorithms for Point Cloud Construction using Digital Projection Patterns," Journ. Comput. and Inform. Sci. Eng. **7** (4), 372–381 (2007).
7. O. K. Yilmaz, S. Ozder, P. Demir, "Two-Dimensional Fringe Projection for Three-Dimensional Shape Measurements by using the CWT Phase Gradient Method," Avtometriya **47** (2), 33–45 (2011) [Optoelectron., Instrum. Data Process. **47** (2), 130–140 (2011)].
8. K. Creath, "Phase-Measurement Interferometry Techniques," Progr. Opt. **26**, 349–393 (1988).

9. V. I. Guzhov and S. P. Il'inykh, *Computer Interferometry* (Izd. NGTU, Novosibirsk, 2004) [in Russian].
10. S. P. Il'inykh and V. I. Guzhov, "A Generalized Decoding Algorithm Interferograms using Phase Stepping," Avtometriya **38** (3), 123–126 (2002).
11. V. I. Guzhov, S. P. Il'inykh, D.S. Khaidukov, and A.R. Vagizov, "Universal Decoding Algorithm," Nauch. Vestn NGTU, **41** (4), 51–58 (2010).
12. C. Guan, L. Hassebrook, and D. Lau, "Composite Structured Light Pattern for Three-Dimensional Video," Opt. Express. **11** (5), 406–417 (2003).
13. D. Ghiglia and M. Pritt, *Two-Dimensional Phase Unwrapping Theory, Algorithms and Software* (John Wiley & Sons, 1998)
14. F. Qiangian, P. M. Meaney, and K. D. Paulsen, "The Multidimensional Phase Unwrapping Integral and Applications to Microwave Tomographical Image Reconstruction," IEEE Trans. Image Process. **15** (11), 3311–3324 (2006).
15. V. I. Guzhov, S. P. Il'inykh, and E. V. Kartavykh, "Systematic Error Correction in Determining the Total Phase in Integer Interferometry," Avtometriya **44** (6), 96–102 (2008) [Optoelectron., Instrum. Data Process. **44** (6), 552–556 (2008)].
16. J. V. Uspensky and M. A. Heaslet, *Elementary Number Theory* (McGraw-Hill, Mew York, 1939).
17. V. I. Guzhov, S. P. Il'inykh, and A. I. Ubert, "Projection Method for Measuring Topography," Nauch. Vestn. NGTU **46** (1), 23–28 (2012).
18. V. I. Guzhov, S. P. Il'inykh, A. R. Vagizov, and R. A. Kuznetsov, "Increasing of Accuracy of Definition of Coordinates in Robotic Vision," in *Proc. of the 2nd Russian-Indian Joint Workshop on Computational Intelligence and Modern Heuristics in Automation and Robotics* (NSTU, Novosibirsk, 2011), pp. 184–187.